Molecular Crystals and Liquid Crystals

ISSN: 1542-1406 (Print) 1563-5287 (Online) Journal homepage: http://www.tandfonline.com/loi/gmcl20

Analysis of hydrogen-bonded liquid crystals formed between nitro-substituted benzoic acid and p-n-alkyloxy benzoic acids

N. Pongali Sathya Prabu & M.L.N. Madhu Mohan

To cite this article: N. Pongali Sathya Prabu & M.L.N. Madhu Mohan (2016) Analysis of hydrogen-bonded liquid crystals formed between nitro-substituted benzoic acid and p-n-alkyloxy benzoic acids, Molecular Crystals and Liquid Crystals, 631:1, 47-63, DOI: 10.1080/15421406.2016.1149019

To link to this article: http://dx.doi.org/10.1080/15421406.2016.1149019

MOLECULAR CRYSTALS AND LIQUID CRYSTALS
2016, VOL. 631, 47–63
http://dx.doi.org/10.1080/15421406.2016.1149019

Taylor & Francis
Taylor & Francis Group

Analysis of hydrogen-bonded liquid crystals formed between nitro-substituted benzoic acid and p-n-alkyloxy benzoic acids

N. Pongali Sathya Prabu and M.L.N. Madhu Mohan

Liquid Crystal Research Laboratory (LCRL), Bannari Amman Institute of Technology Sathyamangalam, India

ABSTRACT

A novel series of hydrogen-bonded liquid crystals (HBLC) comprising of eight mesogenic complexes are formed between 3-Nitrobenzoic acid (NBAO) and p-n-alkyloxy benzoic acids (nBAO). The formation of inter molecular hydrogen bonding is evinced through FTIR spectra. Mesogenic phases are confirmed through the textural observations made by Polarizing Optical Microscope (POM) and their transition temperatures are correlated with the data obtained from Differential Scanning Calorimetry (DSC) studies. Phase diagram is constructed from POM and DSC studies. Odd–even effect has been evinced in the transition temperature and enthalpy values corresponding to the smectic C phase transition. Optical tilt angle in smectic C phase is fitted to a power law which reveals that the temperature variation of the tilt angle measurement follows the Mean Field theory predicted value. Thermal stability factor for the individual phase is also elucidated. Dielectric dispersion curves are obtained for the complexes exhibiting nematic phase.

KEYWORDS

Hydrogen-bonded liquid crystals; Tilt angle; Dielectric dispersion curves

1. Introduction

Liquid crystalline materials scored tremendous impact among the scientific society in the recent days as their usage in the fabrication of the display devices becomes an inevitable one due to the anisotropy properties exhibited by them [1–3]. Technology boom, distinct response and the multifold usage to the society made these materials a frontier in the field of science and engineering applications [4–5]. Thermotropic liquid crystalline materials a broad branch of this soft condensed matter gained more importance as the thermal energy persisting within the chemical systems favors the phase formation [6–7] which is the prime utility of the material synthesized to be implemented in the fabrication of any liquid crystal display device. This core ingredient is achieved in numerous ways among which hydrogen-bonded liquid crystals (HBLC) forms the ease one. Molecular reorganization, self-assembling of the chemical moieties and the complimentary bond existing between them favors the mesogenic phase formation irrespective of the nature of the ingredients considered [8–9]. Lower bonding and activation energies exhibits a profound influence on the thermal properties exhibited by these HBLC systems [10–11]. Isotropic temperature where the mesogenic molecules becomes completely liquid in nature, enthalpy values that a particular system possess and the mesomorphic phase behavior observed completely in the complexes are some of the parameters which are influenced by the thermal property of the systems prepared. Kato [12] and Paleos [3] are the

CONTACT M.L.N. Madhu Mohan mln.madhu@gmail.com, lakshminarayanammohan@bitsathy.ac.in
Color versions of one or more of the figures in the article can be found online at www.tandfonline.com/gmcl.

two pioneer groups that are expertized in synthesizing various HBLC and investigating their properties for the fruitfulness applications.

Literature survey of the past insists that it is sufficient if one of the chemical ingredient used in the synthesis route i.e., either the proton donor or the electron acceptor exhibits the mesogenic property to produce a mesogenic complex [13, 14]. Experimental results proved a step ahead of inducing the mesogenic nature between two chemical systems which are non mesogenic in nature [15–17].

In the wake of the rich literature available for the functional groups and their diversified utility as explained above, an attempt is made and achieved in developing a new liquid crystalline system between two chemical systems which are mesogenic in nature. Symmetrical systems viz. benzoic acids (NBAO+nBAO) are considered for the investigation, where "N" refers to the nitro group attached to the metaposition of the aromatic ring in order to promote the transverse dipole moment of the complexes formed. Optical, thermal, and the dielectrical properties exhibited by these systems are investigated in the present article and the conclusions obtained are discussed elaborately in the forth coming sections.

2. Experimental

Optical textural observations are made with a Nikon polarizing microscope equipped with Nikon digital CCD camera system with 5 mega pixels and 2560*1920 pixel resolutions. The liquid crystalline textures are processed, analyzed, and stored with the aid of NIS imaging software system. The temperature control of the liquid crystal cell is equipped with Instec HCS402-STC 200 temperature controller (Instec, USA) to a temperature resolution of $\pm$ 0.1°C. This unit is interfaced to computer by IEEE –STC 200 to control and monitor the temperature. The transition temperatures and corresponding enthalpy values are obtained by DSC (Shimadzu DSC-60, Japan). FTIR spectra is recorded (ABB FTIR MB3000) and analyzed with the MB3000 software. Dielectric studies are performed by Impedance analyzer (LF 4192A, Agilent, USA). p-n-alkyloxy benzoic acids and 3- Nitro benzoic acid are supplied by Sigma Aldrich, (Germany) and all the solvents used are of High Performance Liquid Chromatography (HPLC) grade.

2.1 Synthesis of the hydrogen-bonded complexes

Alkyloxy benzoic acids referred as (nBAO) with carbon number pentyl to dodecyl formed hydrogen bond with 3-Nitrobenzoic acid referred as (NBAO) yielding eight hydrogen-bonded homologues represented as NBAO+5BAO, NBAO+6BAO, NBAO+7BAO, NBAO+8BAO, NBAO+9BAO, NBAO+10BAO, NBAO+11BAO, and NBAO+12BAO. Reported [18] synthetic procedure is adopted for synthesizing the present homologous series. The atomic structure of NBAO+6BAO mesogenic complex is represented as Fig. 1a and the general chemical structure of NBAO+nBAO homologous series is depicted as Fig. 1b.

3. Results and discussion

All the mesogens isolated under the present investigation show a high degree of solubility in coordinating solvents like dimethyl sulfoxide (DMSO) and pyridine. The phase variance exhibited by NBAO+nBAO homologous series is given in Table 1. They also show high thermal and chemical stability when subjected to repeated thermal scans performed during POM and DSC studies.

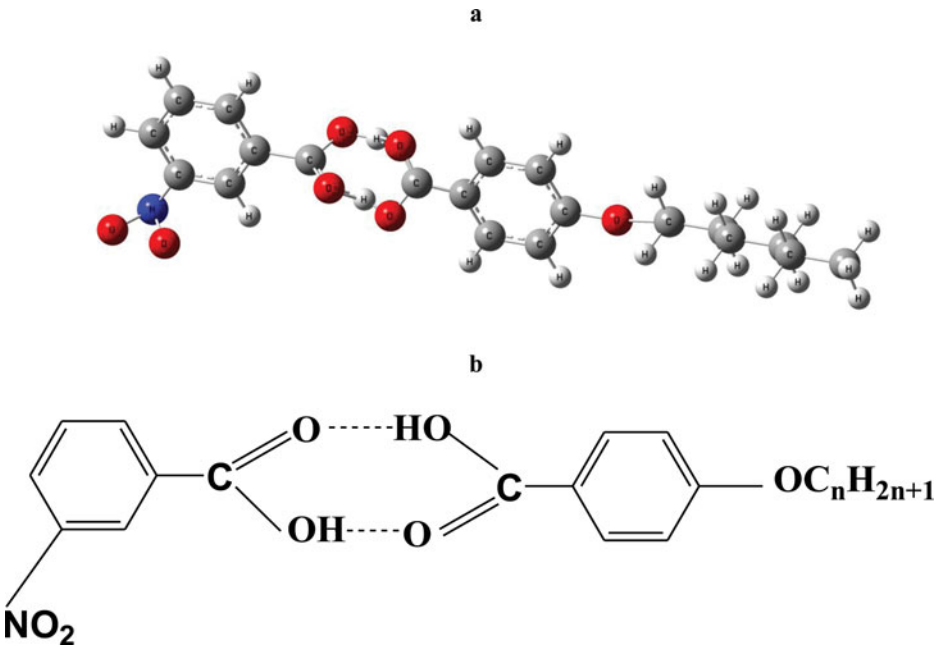

Figure 1. (a) Atomic structure of NBAO+nBAO (b) Chemical structure of NBAO+nBAO (n varies from 5 to 12).

Table 1. Phase transition temperatures and the corresponding enthalpy values obtained for NBAO+nBAO homologous series from DSC thermograms along with the transition temperatures obtained from POM.

Complex & phase variance	Technique	N	X	C	G	K	K_1
NBAO+12BAO NXCG	DSC (h)	#		100.7 (16.14)	91.0 (73.62)		
	DSC (c)	126.5 (9.66)		93.7 (2.11)	76.3 (16.60)	68.3 (22.86)	
	POM (c)	127.5	98.0	94.5	76.9	68.5	
NBAO+11BAO NCG	DSC (h)	#		#	74.6 (29.66)		
	DSC (c)	121.3 (13.64)		82.1 (1.66)	69.2 (25.27)	59.4 (20.93)	
	POM (c)	122.1		82.9	69.7	59.6	
NBAO+10BAO NXCG	DSC (h)	#		98.5 (48.52)	72.5 (15.39)		
	DSC (c)	133.7 (6.13)		95.0 (2.91)	64.3 (22.38)	59.1 (4.99)	
	POM	134.6	102.4	95.4	64.6	59.2	
NBAO+9BAO NCG	DSC (h)	#		#	73.6 (30.97)		
	DSC (c)	122.5 (7.10)		85.3 (0.73)	66.7 (6.72)	63.8 (0.56)	53.2 (3.51)
	POM	123.3		86.1	67.1	64.1	
NBAO+8BAO N	DSC (h)	96.8 (52.15)					
	DSC (c)	119.9 (4.08)				88.9 (1.74)	66.9 (19.00)
	POM	120.4				89.3	
NBAO+7BAO N	DSC (h)	91.5 (34.84)					
	DSC (c)	91.8 (2.85)				76.0 (26.95)	48.1 (0.90)
	POM	92.5				76.5	
N BAO+6BAO G	DSC (h)				97.5 (5.0)		
	DSC (c)				95.6 (18.31)	82.2 (3.63)	
	POM				96.1	82.4	
NBAO+5BAO G	DSC (h)				98.8 (37.73)		61.2 (11.96)
	DSC (c)				93.4 (8.63)	80.4 (30.64)	61.00 (4.39)
	POM				94.1	80.6	

N: Nematic, X: Smectic X, C: Smectic C, G: Smectic G, K: Crystal, K_1: Crystal.
#: Monotropic transition, Enthalpy values in J/g given in parenthesis. h: Heating run, c: Cooling run.

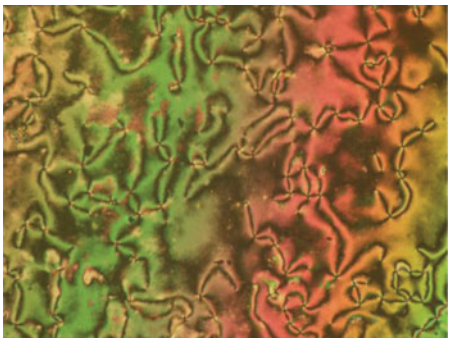

Plate 1. Four brush texture of nematic phase observed in NBAO+8BAO complex.

3.1 Phase variance and identification

The mesogenic phases observed by the various homologues along with their transition temperatures observed both in POM and DSC is represented in Table 1 along with the corresponding enthalpy values obtained for the same in the DSC run. The phases of eight homologues are characterized by POM for textural identification. NBAO+nBAO homologous series exhibits rich phase polymorphism. In all, four liquid crystalline phases have been identified. The orthogonal phase is nematic (plate 1,) while the tilted phases are Smectic X (plate 2 depicting the partially grown smectic X subsiding nematic and plate 3 depicting fully grown smectic X phase), smectic C (plate 4), and smectic G (plate 5) respectively. Smectic X is a new phase which has been identified in two of the longer carbon chain number. This type of smectic ordering has been characterized by various techniques and reported earlier by us [19–25].

In all the complexes, nematic is observed as drop lets and on coalescing it transforms to four brush schlieren texture. Worm like texture is ascribed to the smectic X phase grown. Broken focal conic texture is attributed to the smectic C phase which is present in four of the complexes synthesized. Smooth multi colored mosaic is characteristic texture of smectic G which is noticed in 75% of the complexes prepared. The general phase sequence of 3-Nitro benzoic acid with alkyloxy benzoic acids in cooling and heating run of DSC are shown as:

$$Iso \rightleftharpoons Sm\,G \rightleftharpoons Crystal \quad (\text{NBAO} + 5\text{BAO}, \text{NBAO} + 6\text{BAO})$$
$$Iso \rightleftharpoons \text{N} \rightleftharpoons Crystal \quad (\text{NBAO} + 7\text{BAO}, \text{NBAO} + 8\text{BAO})$$
$$Iso \rightarrow N \rightarrow Sm\,\text{C} \rightleftharpoons Sm\,G \rightleftharpoons Crystal \ (\text{NBAO} + 9\text{BAO}, \text{NBAO} + 11\text{BAO})$$
$$Iso \rightarrow N \rightarrow Sm\,\text{X} \rightleftharpoons Sm\,C \rightleftharpoons Sm\,G \rightleftharpoons Crystal \ (\text{NBAO} + 10\text{BAO}, \text{NBAO} + 12\text{BAO})$$

Single arrows indicate monotropic transitions while double arrows indicate enantiotropic transitions.

3.2 Fourier transform infrared spectroscopy (FTIR)

FTIR spectra for the precursors NBAO, nBAO and for the hydrogen-bonded complexes formed between these two ingredients under present study are recorded in the solid state (KBr) at room temperature. In the pure compounds, carboxylic acid exists in monomeric form and the stretching vibration of C=O is observed at 1760 cm^{-1} [26–29]. When a hydrogen bonding is formed between carboxylic acids it results in lowering of the carbonyl frequency of saturated acids which has been detected in the present hydrogen-bonded complexes also.

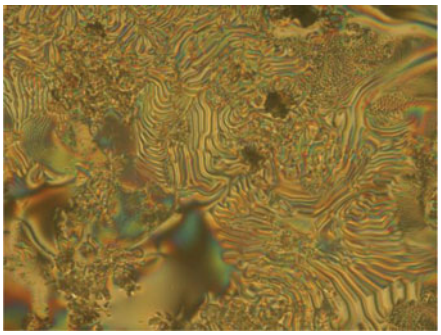

Plate 2. Phase transition from four brush texture of nematic to smectic X phase observed in NBAO+12BAO complex.

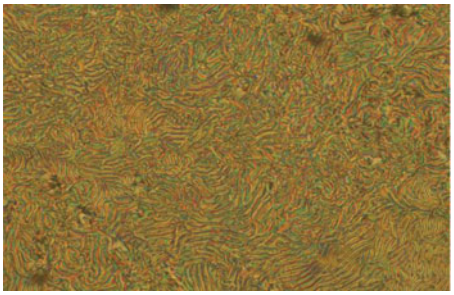

Plate 3. Completely grown worm like texture of smectic X phase observed in NBAO+12BAO complex.

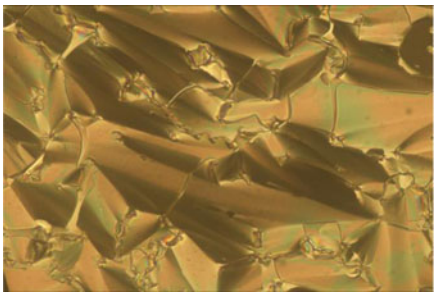

Plate 4. Broken focal conic texture of smectic C phase observed in NBAO+11BAO complex.

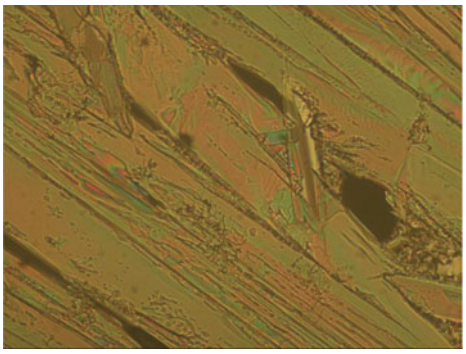

Plate 5. Multi colored smooth mosaic like texture of smectic G phase observed in NBAO+5BAO complex.

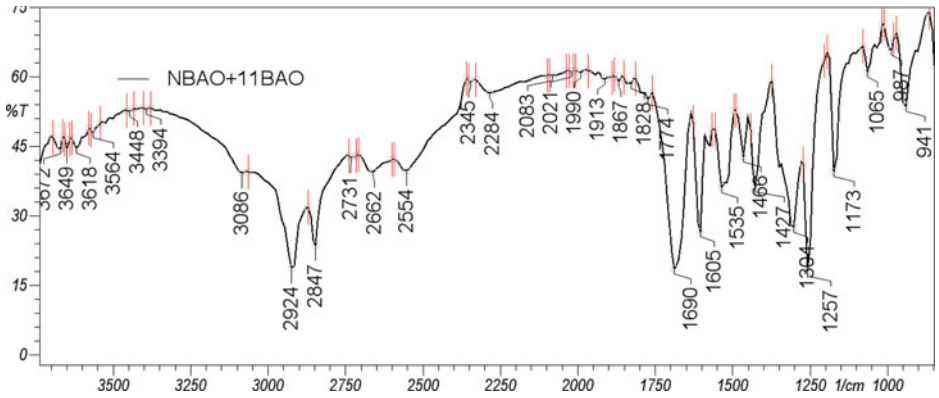

Figure 2. FTIR spectrum of NBAO+11BAO complex.

As a representative case, FTIR spectra of NBAO+11BAO is depicted in Fig. 2 where the corresponding C=O stretching can be noticed at 1690 cm^{-1}. A sharp intense peak observed at 2924 cm^{-1} is attributed to the O-H stretching observed in the intermolecular hydrogen-bonded NBAO+11BAO complex conforming the hydrogen bond formation upon complexation. The C=O and O–H peaks of the entire hydrogen-bonded complexes are listed in Table 2. It can be inferred from Table 2, that the lowering of O-H stretching takes place as the flexible moiety length increases.

3.3 DSC studies

DSC thermograms are obtained in heating and cooling cycle. The sample is heated with a scan rate of 10°C/min and held at its isotropic temperature for two minutes so as to attain thermal stability. The cooling run is performed with a scan rate of 10°C/min. The respective equilibrium transition temperatures and corresponding enthalpy values of the mesogens of the homologous series are listed separately in Table 1. POM studies also confirm these DSC transition temperatures. As a representative case the DSC thermogram for the NBAO+12BAO complex is given in Fig. 3a and the corresponding data is tabulated in Table 1. The cooling thermograms for the entire NBAO+nBAO homologous series is given in Fig. 3b along with the phase transitions.

In the cooling run of DSC thermogram, the NBAO+12BAO complex possesses four distinct peaks. The first peak is observed at 126.5°C with an enthalpy value of 9.66 J/g which is attributed to isotropic to nematic phase transition. The second peak is observed at 93.7°C with an enthalpy value of 2.11 J/g which is attributed to smectic X to smectic C phase transition. The third peak is observed at 76.3°C with an enthalpy value of 16.60 J/g which is attributed to smectic C to smectic G phase transition. The fourth peak is observed at 68.3°C with an

Table 2. FTIR peak assignments observed for OH and COOH stretching in NBAO+nBAO complexes.

NBAO+nBAO	ν $(OH)_{acid}$	$\nu(COOH)_{acid}$
NBAO+5BAO	2955	1682
NBAO+6BAO	2947	1690
NBAO+7BAO	2932	1690
NBAO+8BAO	2932	1690
NBAO+9BAO	2924	1682
NBAO+10BAO	2924	1690
NBAO+11BAO	2924	1690
NBAO+12BAO	2924	1690

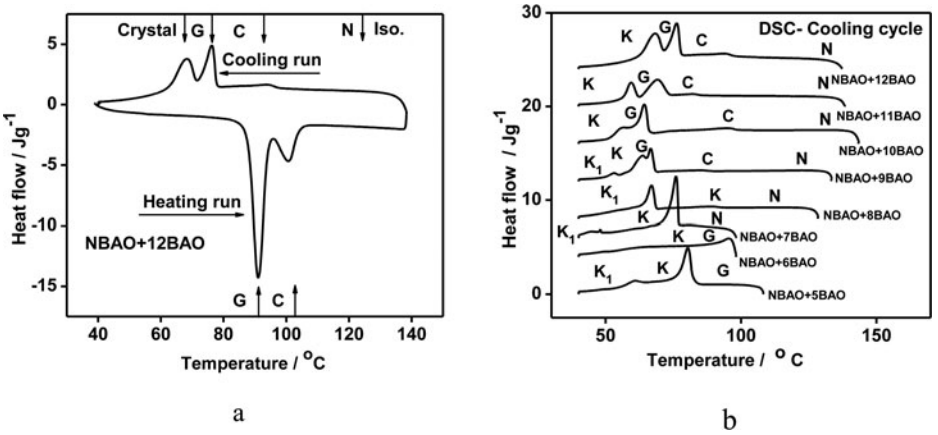

Figure 3. (a) DSC thermogram of NBAO+12BAO complex (b) DSC thermogram of NBAO+nBAO homologous series in cooling run.

enthalpy value of 22.86 J/g which is attributed to smectic G to crystal phase transition. In the heating run of NBAO+12BAO complex, two distinct peaks are noticed. The first peak corresponds to crystal to smectic G phase transition which is observed at 91.0°C possessing an enthalpy value of 73.62 J/g. The second peak corresponds to smectic G to smectic C phase transition which is observed at 100.7°C possessing an enthalpy value of 16.14 J/g. Smectic X to smectic C and smectic C to smectic G phase transitions are observed to be enantiotropic transitions. Isotropic to nematic transition is observed to be monotropic in nature. As the thermal range is minimum for smectic X phase transition, which is not well resolved by DSC, POM data is considered.

3.4 Phase diagram

The phase diagram is constructed from the textural data of the POM studies correlated to the transition temperatures obtained by DSC thermograms. The transition temperature of smectic X is elucidated from POM data as it is not well resolved in DSC thermograms. The phase variance of precursor p-n alkyloxy benzoic acids is reported [30] as nematic, smectic C and smectic G and 3-Nitro benzoic acid exhibits smectic G phase. The homologous series of NBAO+nBAO exhibit rich phase polymorphism as depicted in Fig. 4 which are discussed below:

1. Four phases viz.., nematic, smectic X, smectic C and smectic G are observed in the phase diagram.
2. An interesting feature is inducement of smectic X in the higher ordered even homologues (NBAO+10BAO and NBAO+12BAO) which is sandwiched between traditional nematic and conventional smectic C.
3. Enhancement in the molecular anisotropy for the even carbon numbers lead to the inducement of new smectic X phase.
4. The thermal range of smectic X phase is quite small (less than 10 degrees) and hence it is not well resolved by DSC thermograms.
5. Out of eight mesogenic complexes, four exhibits mono phase variant among which nematic is exhibited by two (NBAO+7BAO and NBAO+8BAO) and smectic G by the other two (NBAO+5BAO and NBAO+6BAO) mesogenic complexes. Phase variance of precursors dominates in the lower order homologous series.

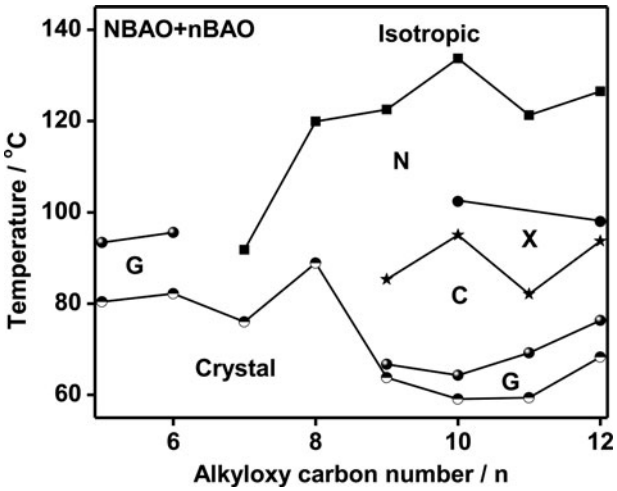

Figure 4. Phase diagram of NBAO+nBAO homologous series

6. Inducement of smectic C originates from nonyloxy carbon number and prevails until the carbon chain length reaches dodecyloxy.
7. High ordered smectic G phase spreads evenly in the homologues with an exemption of NBAO+7BAO and NBAO+8BAO where the traditional nematic phase annihilates completely the smectic G phase.

The phase diagram is further examined in terms of area occupied by mesophase. The area occupied by each of the phase exhibited is mathematically calculated. It is observed that all the four phases viz., nematic, smectic X, smectic C, and smectic G possess an area of 56.97 cm^2, 11.14 cm^2, 26.91 cm^2, and 13.23 cm^2, respectively. Thus the percentage of nematic, smectic X, smectic C, and smectic G in the entire phase diagram is observed to be 52.62%, 10.3%, 24.86%, and 12.22%, respectively.

3.5 Odd–even effect across smectic C to smectic G transition temperatures

Chemical structure of the mesogens contributes to the odd–even effect observed in transition temperatures and enthalpy values possessed by them. In even carbon number mesogens, the nature of the terminal groups attached is to enhance the molecular anisotropy and hence molecular order, whereas in the odd carbon number it has the opposite effect. Increment in carbon chain length is proportional to the flexibility of the structure which leads to the suppression in the odd–even effect. The results of the odd–even effect observed in the present NBAO+nBAO series formed from the hydrogen-bonded complexes are in accordance with the quantitative calculations proposed and reported earlier [31–35].

In the present intermolecular HBLC complexes, 3-Nitrobenzoic acid is considered to be the rigid or core molecule whereas benzoic acids forms the flexible part. The length of the complex varies with increase in the alkyloxy benzoic acid carbon chain. The rich phase polymorphism and the associated enthalpy values exhibited by these complexes (Table 1) with increment of alkyloxy carbon chain length are thus attributed to this part of the chemical structure. Moreover the length (l) of the total HBLC varies with the alkyloxy carbon chain length while the width (d) remains constant. Thus the altering of l/d ratio triggers the phase variance in the homologous series in turn influences the phase transition temperatures and the corresponding enthalpy values. Hence, the rigid cores and l/d ratio plays a vital

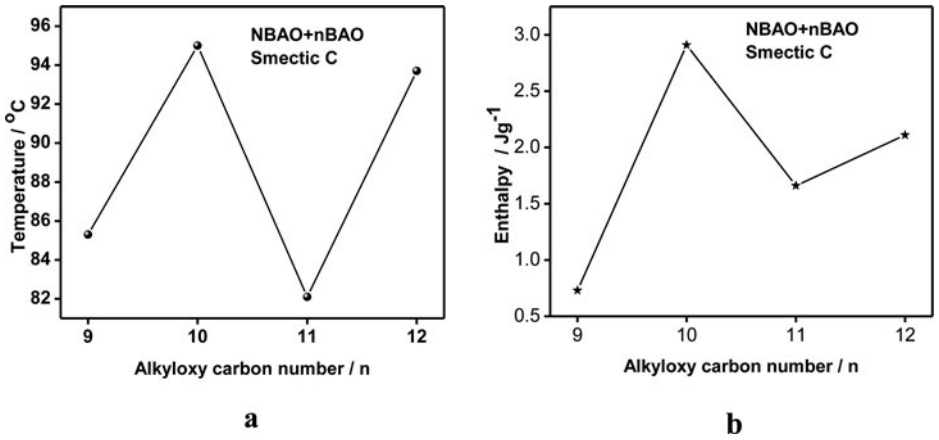

Figure 5. (a) Odd–even effect observed across transition temperatures of NBAO+nBAO homologous series (b) Odd–even effect observed across enthalpy values of NBAO+nBAO homologous series.

role in establishing the pronounced odd–even effect as evinced in the present homologues prepared.

Here, in the present hydrogen-bonded NBAO+nBAO series odd–even effect is noticed across the temperatures and enthalpy values of the smectic C phase transition which is represented in Fig. 5a and 5b respectively. Plots are constructed with the temperature and the corresponding enthalpy values along y-axis and the alkyloxy carbon chain number along *x*-axis. From Fig. 5a and 5b, it can be observed that the magnitudes of the enthalpy values corresponding to the even homologous mole fraction exhibit one type of behavior, while their odd counter parts show a different pattern. In the literature, such behavior has been reported [32] and is referred as odd–even effect.

3.6 Thermal stability

It is reported [36, 37] that when the liquid crystal molecules have two symmetric end chains the phase transition temperatures are higher for the systems. In a symmetric system, the end chains affect the phase transition temperatures as well as the temperature ranges of various phases. The molecular weights of terminal chain could be considered as the measure of balancing and if they are nearly equal, the system is balanced. In other words the system is symmetric about its molecular short axis.

Phase stability is one of the important parameters that govern the utility of the mesogen. In the present case phase stability of nematic is discussed. The term nematic phase stability can be attributed to isotropic to nematic transition temperature as well to the temperature range of nematic phase. It is reasonable to consider both the above factors and define a parameter called stability factor (S). As a representative case the stability factor for nematic (S_N) is given by

$$S_N = T_{mid} * \Delta T_N$$

T_{mid} is the mid nematic temperature and $\Delta T_{N,}$ the nematic thermal range. In this manner, the thermal stability of smectic C and smectic G exhibited by different homologues are calculated along with nematic phase and are tabulated in Table 3 and represented as Fig. 6. It can be noted from the Table 3 and Fig. 6 that with an exception of NBAO+7BAO, the thermal stability factor of nematic exhibits odd–even effect. A similar trend is noticed for smectic C phase also. The

Table 3. Thermal stability factor obtained for NBAO+nBAO complexes in different phases.

Complex	N	X	C	G
NBAO+12BAO	3199	412	1479	578
NBAO+11BAO	3987	–	976	630
NBAO+10BAO	3695	730	2445	321
NBAO+9BAO	3865	–	1414	189
NBAO+8BAO	3236	–	–	–
NBAO+7BAO	1326	–	–	–
NBAO+6BAO	–	–	–	1191
NBAO+5BAO	–	–	–	1130

N: Nematic, X: Smectic X, C: Smectic C, G: Smectic G.

increase in chain length prominently induced the above said phenomenon. Thus the highest thermal stability factor for nematic is recorded for NBAO+11BAO with a magnitude of 3987. Smectic X has highest magnitude (730) of thermal stability factor for NBAO+11BAO and smectic G exhibited highest magnitude of thermal stability factor for NBAO+6BAO.

3.7 Optical tilt angle measurement

The optical tilt angle has been experimentally measured in smectic C phase by optical extinction method [38] of all the members of the present NBAO+nBAO homologous series exhibiting smectic C phase. Fig. 7 depicts such variation of optical tilt angle with temperature for NBAO+nBAO (where $n = 9$to 12) series. The theoretical fit obtained from the Mean Field theory is denoted by the solid line. It is observed that the tilt angle increases with decreasing temperature and attains a saturation value. Attainment of fair magnitudes of the tilt angle are attributed to the direction of the soft covalent hydrogen-bond interaction which spreads along molecular long axis with finite inclination [39].

Tilt angle is a primary order parameter [40] and the temperature variation is estimated by fitting the observed data of θ (T) to the relation

$$\theta(\mathrm{T})\alpha(\mathrm{TC}-\mathrm{T})^{\beta} \tag{1}$$

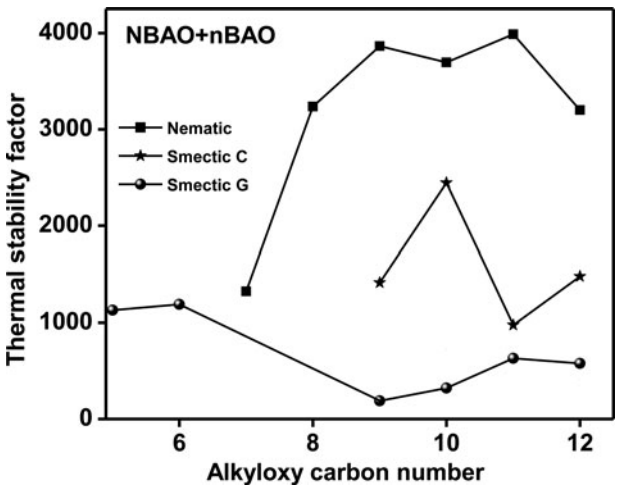

Figure 6. Thermal stability factor obtained for different phases in NBAO+nBAO homologues series.

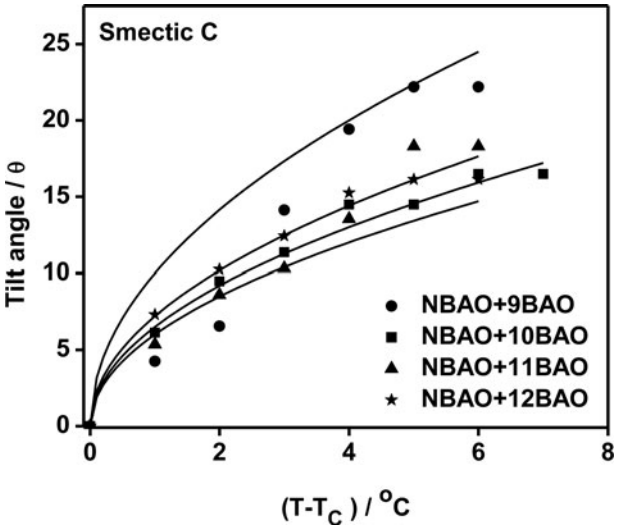

Figure 7. Optical tilt angle measurements made in smectic C phase of NBAO+nBAO homologous series

The critical exponent β value estimated by fitting the data of θ (T) to the above equation (1) is found to be 0.50 to agree with the Mean Field prediction [41, 42]. The solid lines in the Fig. 7 depict the fitted data for various mesogens. Further, the agreement of magnitude of β (0.5) with Mean Field value (0.5) infers the long-range interaction of transverse dipole moment for the stabilization of tilted smectic C phase.

The highest magnitude of tilt angle in smectic C phase is observed to be 23° for NBAO+9BAO, while the lowest, is observed to be 14° for NBAO+10BAO. This fair magnitude of the tilt angle is attributed to the enhanced orientational disorder introduced by the lengthy flexible part of the molecule, contributing to the ordered smectic C phase.

3.8 Dielectric studies

Empty conducting cell of 10 micron spacing (Instec, USA) is calibrated with temperature (30°C to 150°C) and frequency (5Hz to 13 MHz) by a known substance (benzene) to calculate the leads capacitance.

3.8.1 Dielectric relaxations

Dielectric dispersion i.e. frequency variation of dielectric loss exhibited by NBAO+nBAO complexes is studied at different temperatures in nematic phase in the frequency range of 5 Hz to 13 MHz. An impedance analyzer (Agilent 4192A LF, Santa Clara, USA) is operated with $1V_{P\text{-}P}$ oscillating signal with zero bias field. Relative permittivity ε'_r (ω) and dielectric loss ε'' (ω) are calculated by the following equations

$$^*\varepsilon'_r(\omega) = \varepsilon'_r(\omega) - j\varepsilon''(\omega)$$
$$\varepsilon'_r(\omega) = [C_{LC} - C_{leads}]/[C_{empty} - C_{leads}]$$
$$^*\varepsilon' r(\omega) = \mathrm{Tan}\delta(\omega)^*\varepsilon_r(\omega)$$

To detect the possible relaxation in NBAO+nBAO complexes, the mesogen is scanned in the frequency range of 5 Hz to 13 MHz at different temperatures in the orthogonal and tilted phases of the corresponding complex.

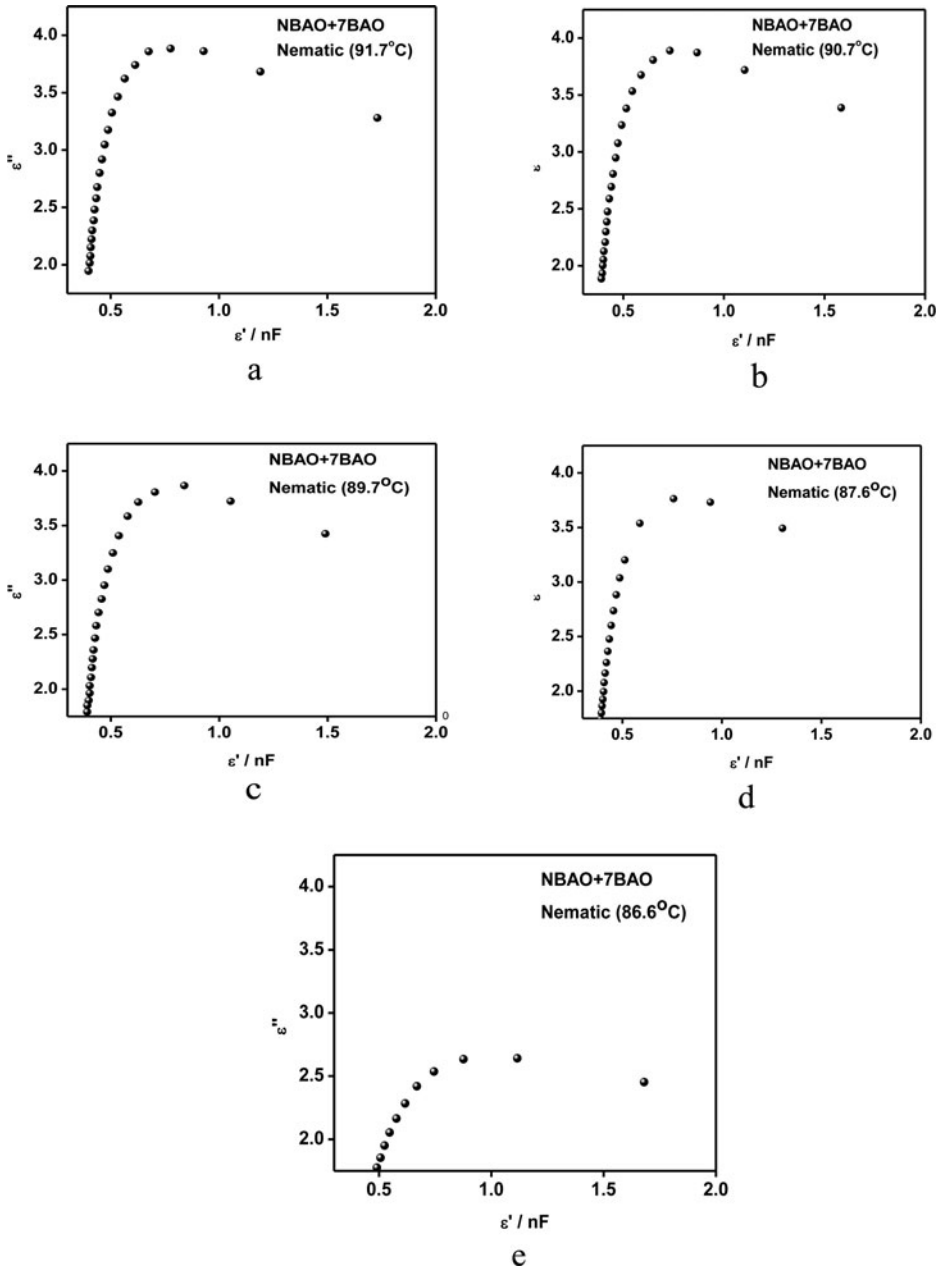

Figures 8a–e. Dielectric dispersion curves obtained for NBAO+7BAO complex in nematic phase at different temperatures.

The observed variation of dielectric loss with capacitance at a fixed temperature is recorded in nematic phase and plotted which is referred as dispersion curves (Figures 8a–8e). From the dispersion curves the magnitude of the dielectric loss is shifted with temperature. The distribution parameter is calculated from the dispersion curves obtained for the complexes and the data is tabulated as Table 4. Such a asymmetric non-Debie's type of off-centered dispersion is studied by Cole-Davidson theory [43–45] and given by the expressions,

$$\varepsilon''(\omega) = \{\varepsilon_\infty - [(\Delta\omega)]/[1 + (j\omega t)^{1-\alpha}$$

Table 4. Values of relaxation frequency and corresponding temperature along with the distribution parameter value for NBAO+nBAO complexes.

Complex	T(°C)	f_r (Hz)	ε'' max	α (rad)
NBAO+7BAO Nematic	91.7	12000	3.889	0.0523
	90.7	11000	3.884	0.0697
	89.7	10000	3.866	0.0872
	87.6	8000	3.73	0.1046
	86.6	6000	2.641	0.1744
NBAO+8BAO Nematic	119.8	5000	4.431	0.4361
	116.8	5500	4.323	0.5407
	113.8	6000	4.262	0.6977
	110.8	7000	4.002	0.7326
	107.8	7500	3.689	0.8722
	104.8	8000	3.48	0.9071
	101.8	8500	2.847	0.9245
NBAO+9BAO Nematic	121.7	3100	3.044	0.0872 0.1570
	120.7	3000	3.042	0.1046 0.1744
	119.7	2900	3.036	0.0872 0.1918
	118.7	2800	3.033	0.1046 0.2093
	117.7	2700	3.01	0.1221 0.2267
	116.7	2600	2.979	0.1395 0.2616
	115.7	2500	2.897	0.1570 0.2791
NBAO+10BAO Nematic	132.8	6226	2.776	0.3488
	131.8	5369	2.77	0.3663
	130.8	5264	2.769	0.3837
	129.8	4298	2.727	0.4186
	128.8	4145	2.726	0.4535
NBAO+11BAO Nematic	120.4	6079	3.444	0.1570
	119.4	5384	3.352	0.1744
	118.4	5187	3.33	0.2093
	117.4	5169	3.326	0.2616
	116.4	4938	3.321	0.2791
	115.4	4886	3.310	0.2965
	114.4	4835	3.271	0.3140
	113.4	4097	3.237	0.3488
	112.4	4045	3.217	0.4012
	111.4	3994	3.164	0.4186
	110.4	3205	3.114	0.4186
	109.4	3153	3.05	0.4361
	108.4	3110	2.986	0.4535
NBAO+12BAO Nematic	125.6	2177	4.54	0.3314
	124.6	1994	4.37	0.3488
	123.6	1967	3.895	0.3663
	122.6	1939	3.696	0.4186
	121.6	1912	3.429	0.4361
	119.6	1015	2.922	0.4884

where

$\Delta\varepsilon = (\varepsilon_{o\text{-}}\ \varepsilon_{\infty})$ = the dielectric increment (strength)

$\omega = 2\pi f$ (where f is the frequency of AC signal)

τ = relaxation time i.e. $1/f_r$

α = the distribution parameter (or degrees of freedom) to estimate the influence of environment of dipoles and its fixation in the molecular frame during the reorientation to the field.

3.8.2 Dielectric relaxations in nematic phase of NBAO+7BAO homologous series

The dielectric relaxations in NBAO+7BAO complex have been investigated in the entire thermal span of nematic phase (91.8°C to 76°C) at five temperatures namely 91.7°C, 90.7°C, 89.7°C, 87.6°C and 86.6°C, respectively. The corresponding dispersion curves are illustrated

in Figures 8a to 8e which are classified as Cole-Davidson relaxations process. From the dielectric dispersion curves, the individual relaxation frequencies are calculated.

In this complex, the magnitude of dielectric loss decreases with decrement of temperature while the relaxation process is not completely suppressed. The relaxation frequency is 12,000 Hz at 91.7°C with ε'' value of 3.889. The relaxation frequency shifted to 6000 Hz as the temperature is decreased to 86.6°C with a ε'' value of 2.641.Thus the relaxation frequency is proportional to the temperature in this phase.

The distribution parameter α has been calculated for each relaxation observed at different temperatures. The values of relaxation frequency, temperature and distribution parameter are listed in Table 4.

3.8.3 Dielectric relaxations in nematic phase of NBAO+8BAO homologous series

Dielectric relaxations in NBAO+8BAO complex have been investigated in the entire thermal span of nematic phase (119.9°C to 88.9°C) at seven temperatures namely 119.8°C, 116.8°C, 113.8°C, 110.8°C, 107.8°C, 104.8°C, and 101.8°C, respectively. In this complex also the magnitude of dielectric loss decreases with decrement of temperature while the relaxation process is not completely suppressed. The relaxation frequency is 5000 Hz at 119.8°C with ε'' value of 4.431. The relaxation frequency shifted to 8500 Hz as the temperature is decreased to 101.8°C with a ε'' value of 2.847. Thus this complex exhibits anomalous dielectric behavior which means the magnitude of the relaxation frequency increase with the decrement of temperature. The distribution parameter α has been calculated for each relaxation observed at different temperatures and is tabulated as Table 4.

3.8.4 Dielectric relaxations in nematic phase of NBAO+9BAO homologous series

Dielectric relaxations in NBAO+9BAO complex have been investigated in the entire thermal span of nematic phase (122.5°C to 85.3°C) at seven temperatures namely 121.7°C, 120.7°C, 119.7°C, 118.7°C, 117.7°C, 116.7°C, and 115.7°C. In this complex also the magnitude of dielectric loss decreases with decrement of temperature while the relaxation process is not completely suppressed. The relaxation frequency is 3100 Hz at 121.7°C with ε'' value of 3.044. The relaxation frequency shifted to 2500 Hz as the temperature is decreased to 115.7°C with a ε'' value of 2.897. Thus the relaxation frequency is proportional to the temperature in this phase. The distribution parameter α has been calculated for each relaxation observed at different temperatures and is tabulated as Table 4. In addition to the above relaxation mode, another type of relaxation called double or multiple relaxations have been noticed (Figures 9a–9g). Reasons for such kind of occurrence are the transverse dipoles existing within the flexible chemical moieties formed through hydrogen bonding. The contribution of these dipoles is comparatively low with respect to the longitudinal counterparts. This indicates that the linking group in the central core of the mesogenic moiety is more rigidly fixed in the molecular frame than the end chains which are free to rotate.

3.8.5 Dielectric relaxations in nematic phase of NBAO+10BAO homologous series

NBAO+10BAO complex possess rich thermal span of nematic phase (133.7°C to 95°C) and the dielectric relaxations are obtained in the same phase at five temperatures namely 132.8°C, 131.8°C, 130.8°C, 129.8°C, and 128.8°C. From the dielectric dispersion curves, the individual relaxation frequencies are calculated. In this complex, the magnitude of dielectric loss decreases with decrement of temperature while the relaxation process is not completely suppressed. The relaxation frequency is 6226 Hz at 132.8°C with ε'' value of 2.776. The relaxation frequency shifted to 4145 Hz as the temperature is decreased to 128.8°C with a ε'' value

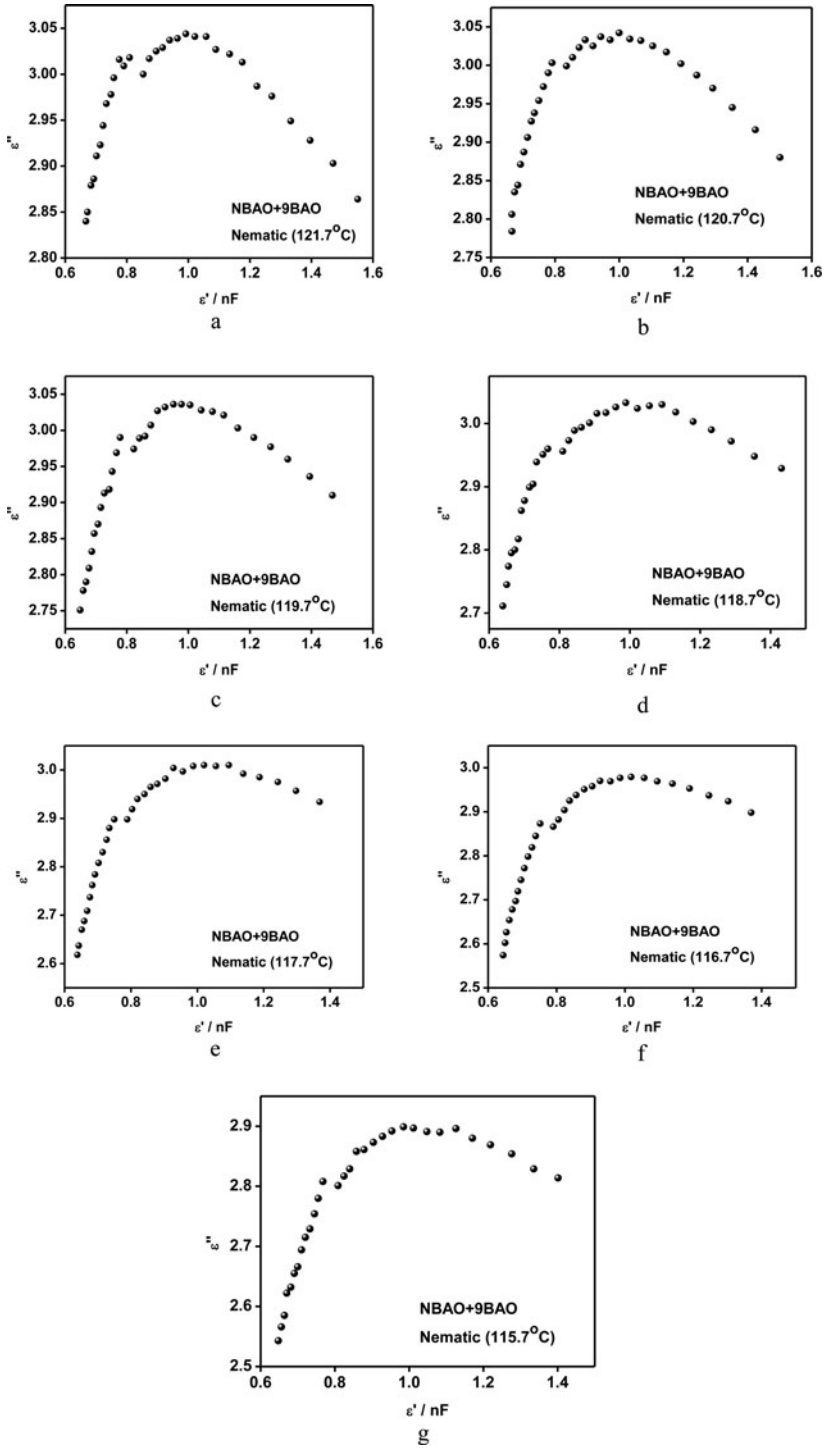

Figures 9a–g. Double relaxation dispersion curves obtained for NBAO+9BAO complex in nematic phase at different temperatures.

of 2.726.Thus the relaxation frequency is proportional to the temperature in this phase. The distribution parameter α has been calculated for each relaxation observed at different temperatures. The values of relaxation frequency, temperature and distribution parameter are listed in Table 4.

3.8.6 Dielectric relaxations in nematic phase of NBAO+11BAO homologous series

In the entire thermal span of nematic phase (121.3°C to 82.1°C) at thirteen temperatures namely 120.4°C, 119.4°C, 118.4°C, 117.4°C, 116.4°C, 115.4°C, 114.4°C, 113.4°C, 112.4°C, 111.4°C, 110.4°C, 109.4°C, and 108.4°C, the dielectric dispersion curves of NBAO+11BAO complex have been studied. From the dielectric dispersion curves, the individual relaxation frequencies are calculated. In this complex also the magnitude of dielectric loss decreases with decrement of temperature while the relaxation process is not completely suppressed. The relaxation frequency is 6079 Hz at 120.4°C with ε'' value of 3.444. The relaxation frequency shifted to 3110 Hz as the temperature is decreased to 108.4°C with a ε'' value of 2.986.Thus the relaxation frequency is proportional to the temperature in this phase. The distribution parameter α has been calculated for each relaxation observed at different temperatures. The values of relaxation frequency, temperature and distribution parameter are listed in Table 4.

3.8.7 Dielectric relaxations in nematic phase of NBAO+12BAO homologous series

The dielectric dispersion curves are obtained for NBAO+12BAO complex in the entire thermal span of nematic phase (126.5°C to 93.7°C) at six temperatures namely 125.6°C, 124.6°C, 123.6°C, 122.6°C, 121.6°C, and 119.6°C respectively. From the dielectric dispersion curves, the individual relaxation frequencies are calculated. In this complex also the magnitude of dielectric loss decreases with decrement of temperature while the relaxation process is not completely suppressed. The relaxation frequency is 2177 Hz at 125.6°C with ε'' value of 4.54. The relaxation frequency shifted to 1015 Hz as the temperature is decreased to 119.6°C with a ε'' value of 2.922.Thus the relaxation frequency is proportional to the temperature in this phase. The distribution parameter α has been calculated for each relaxation observed at different temperatures. The values of relaxation frequency, temperature and distribution parameter are listed in Table 4.

4. Conclusions

a) A successful characterization of inter HBLCs formed between alkyloxy benzoic acids (nBAO) and 3-Nitrobenzoic acid (NBAO) is studied.
b) A new smectic ordering smectic X is observed in the higher even homologues.
c) Odd–even effect is evinced across the transition temperatures and enthalpy values of smectic C phase transition.
d) Tilt angle measurement is made in smectic C phase and the experimental data is fitted to the critical exponent value derived from Mean Field theory.
e) Dielectric dispersion curves along with multiple relaxations are obtained in nematic phase of the NBAO+nBAO homologous series and discussed.

Acknowledgments

The authors acknowledge the financial support rendered by BRNS-DAE, Mumbai, vide 2012/34/35/BRNS. Infrastructural support provided by Bannari Amman Institute of Technology is gratefully acknowledged.

References

[1] Goodby, J. W. (2011). *Liq. Cryst.*, *11*, 1363.
[2] Kato, T., Mizoshita, N., & Kanie, K. (2001). *Micromole. Rapid. Commun.*, *22*, 797.
[3] Paleos, C. M., & Siourvas, D. T. (2001). *Liq. Cryst.*, *28*, 1127.
[4] Beginn, U. (2003). *Prog. Polym Sci.*, *28*, 1049.
[5] Adhikari, B., & Paul, R. (1996). *Phase. Transit.*, *56*, 153.
[6] Navard, P., & Cox, R. (1984). *Mol. Cryst. Liq. Cryst.*, *102*, 261.
[7] Pongali Sathya Prabu, N., & Madhu Mohan, M. L. N. (2012). *Mol. Cryst. Liq. Cryst.*, *557*, 144.
[8] Kato, T., & Frechet, J. M.J. (1989). *J. Am. Chem. Soc.*, *111*, 8533.
[9] Kato, T., Kihara, H., Uryu, T., Ujiie, S., Iimura, K., Frechet, J. M. J., & Kumar, U. (1993). *Ferroelectrics.*, *148*, 161.
[10] Kihara, H., Kato, T., Uryu, T., & Frechet, J. M. J. (1996). *Chem. Mater.*, *8*, 961.
[11] Kato, T., & Frechet, J. M. J. (1989). *Macromolecules.*, *22*, 3818.
[12] Kumar, U., Kato, T., & Frechet, J. M. J. (1992). *J. Am. Chem. Soc.*, *114*, 6630.
[13] Tian, Y. Q., He, X., Zhao, Y. Y., Tang, X. Y., Jin Li, T., & Huang, X. M. (1998). *Mol. Cryst. Liq. Cryst.*, *309*, 19.
[14] Swathi, P., Kumar, P. A., Pisipati, V. G. K. M., Rajeshwari, A. V., Sreehari Sastry, S., & Murthy, P. N. (2002). *Z. Natur. Forsch.*, *57a*, 797.
[15] Kang, S. K., & Samulski, E. T. (2000). *Liq.Cryst.*, *27*, 371.
[16] Hentrich, F., Diele, S., & Tschierske, C. (1994). *Liq.Cryst.*, *17*, 827.
[17] Kobayashi, Y., & Mtsunage, Y. (1987). *Bull. Chem. Soc. Jpn.*, *60*, 3515.
[18] Kato, T., & Mizoshita, N. (2002). *Curr. Opin. Solid. State. Mater. Sci.*, *6*, 579.
[19] Kavitha, C., Pongali Sathya Prabu, N., & Madhu Mohan, M. L. N. (2012). *Physica B.*, *407*, 859.
[20] Pongali Sathya Prabu, N., & Madhu Mohan, M. L. N. (2012). *Mol. Cryst. Liq. Cryst.*, *569*, 72.
[21] Pongali Sathya Prabu, N., Vijayakumar, V. N., & Madhu Mohan, M. L. N. (2011). *J. Mol. Str.*, *994*, 387.
[22] Kavitha, C., & Madhu Mohan, M. L. N. (2012). *J.. Phy. Chem. Solids.*, *73*, 1203.
[23] Kavitha, C., Pongali Sathya Prabu, N., & Madhu Mohan, M. L. N. (2012). *Phase. Transit.*, *85*, 973.
[24] Pongali Sathya Prabu, N., & Madhu Mohan, M. L. N. (2013). *Phase. Transit.*, *86*, 339.
[25] Pongali Sathya Prabu, N., & Madhu Mohan, M. L. N. (2013). *J. Thermal. Anal. Calorim.*, *113*, 811.
[26] Kato, T., & Uryu, T., (1993). *Liq. Cryst.*, *14*, 1311.
[27] Cook, A. G., Baumeister, U., & Tschierske, C. (2005). *J. Mater. Chem.*, *15*, 1708.
[28] Nakamoto, K. (1978). *Infrared and Raman Spectra of Inorganic and Co-ordination Compounds*, Interscience, New York.
[29] Pavia, D. L., Lampman, G. M., & Kriz, G. S. *Introduction to Spectroscopy*, Sanat printers: India.
[30] Vijayakumar, V. N., & Madhu Mohan, M. L. N. (2010). *Mol. Cryst. Liq. Cryst.*, *524*, 54.
[31] Marcelja, S. (1973). *Solid. State. Commun.*, *13*, 759.
[32] Chandrasekhar, S. *Liquid Crystals*, Cambridge University Press: New York, 1977.
[33] Thoen, J., Cordoyiannis, G., & Glorieux, C. (2009). *Liq. Cryst.*, *36*, 66.
[34] Marcelja, S. (1974). *J. Chem. Phys.*, *60*, 3599.
[35] Senthil, S., Ramesh babu, K., & Wu, S. L. (2006). *J. Mol. Struct.*, *783*, 215.
[36] Smith, G. W., & Gardlund, Z. G. (1973). *J. Chem. Phys.*, *59*, 3214.
[37] Osman, Z. (1976). *Z. Naturforsch.*, *31b*, 801.
[38] Noot, C., Perkins, S. P., & Coles, H. J. (2000). *Ferroelectrics.*, *244*, 331.
[39] Srinivasulu, M., Satyanarayan, P. V. V., Kumar, P. A., & Pisipati, V. G. K. M. (2002). *Z .Naturforsch. A. Phy Sci.*, *56A*, 685.
[40] Madhu Mohan, M. L. N., Arunachalam, B., & Arravind Sankar, C. (2008). *Metal. Mater .Trans. A.*, *39*, 1192.
[41] Madhu Mohan, M. L. N., Arunachalam, B., & Arravind Sankar, C. (2008). *Z. Naturforsch. A. Phy Sci.*, *63A*, 435.
[42] Madhu Mohan, M. L. N., & Pisipati, V. G. K. M. (2000). *Liq. Cryst.*, *26*, 1609.
[43] Hills, N. E., Wanghan, W. E., Price, A. H., & Davies, M. (1969). *Dielectric Properties and Molecular Behavior*, Vannostrand: New York.
[44] Jonscher, A. H., (1983). *Dielectric relaxation in solids*, Chelsea Dielectric Press: London.
[45] Cole, R. H. (1941). *J. Chem. Phys.*, *9*, 341.